Low Renal Mineralocorticoid Receptor Expression at Birth Contributes to Partial Aldosterone Resistance in Neonates

Laetitia Martinerie, Say Viengchareun, Anne-Lise Delezoide, Francis Jaubert, Martine Sinico, Sophie Prevot, Pascal Boileau, Geri Meduri, and Marc Lombès

Institut National de la Santé et de la Recherche Médicale (L.M., S.V., G.M., M.L.), Unité 693, Le Kremlin-Bicêtre F-94276, France; Université Paris-Sud 11 (L.M., S.V., G.M., M.L.), Faculté de Médecine Paris-Sud, Unité Mixte de Recherche-S693, Le Kremlin-Bicêtre F-94276, France; Université Paris-Diderot et Assistance Publique-Hôpitaux de Paris (A.-L.D.), Hôpital Robert Debré, Service de Biologie du Développement, Paris F-75019, France; Assistance Publique-Hôpitaux de Paris (F.J.), Hôpital Necker-Enfants Malades, Service d'AnatomoPathologie, Paris F-75015, France; Centre Hospitalier Intercommunal de Créteil (M.S.), Service d'AnatomoPathologie, Créteil F-94010, France; Assistance Publique-Hôpitaux de Paris, Hôpital Antoine Béclère, Service d'AnatomoPathologie (S.P.) et de Pédiatrie et Réanimation Néonatales (P.B.), Clamart F-92141, France; and Assistance Publique-Hôpitaux de Paris, Hôpital de Bicêtre, Service de Pharmacogénétique, Biochimie Moléculaire et Hormonologie (G.M.) et d'Endocrinologie et Maladies de la Reproduction (M.L.), Le Kremlin Bicêtre F-94275, France

The human neonatal period is characterized by renal immaturity with impaired capacity to regulate water and sodium homeostasis, resembling partial aldosterone resistance. Because aldosterone effects are mediated by the mineralocorticoid receptor (MR), we postulated that this hormonal unresponsiveness could be related to low MR expression in the distal nephron. We measured aldosterone and renin levels in umbilical cord blood of healthy newborns. We used quantitative real-time PCR and immunohistochemistry to analyze the expression of MR and key players of the mineralocorticoid signaling pathway during human and mouse renal development. High aldosterone and renin levels were found at birth. MR mRNA was detected in mouse kidney at d 16 postcoitum, peaking at d 18 postcoitum, but its expression was surprisingly very low at birth, rising progressively afterward. Similar biphasic temporal expression was observed during human renal embryogenesis, with a transient expression between 15 and 24 wk of gestation but an undetectable immunoreactive MR in late gestational and neonatal kidneys. This cyclic MR expression was tightly correlated with the evolution of the 11β-hydroxysteroid dehydrogenase type 2 and the epithelial sodium channel α-subunit. In contrast, glucocorticoid and vasopressin receptors and aquaporin 2 followed a progressive and sustained evolution during renal maturation. Our study provides the first evidence for a low renal MR expression level at birth, despite high aldosterone levels, which could account for compromised postnatal sodium handling. Elucidation of regulatory mechanisms governing MR expression should lead to new strategies for the management of sodium waste in preterms and neonates. (*Endocrinology* 150: 4414–4424, 2009)

In mammals, sodium and water homeostasis is mainly controlled by the kidney. In human neonates, the kidney exhibits a certain degree of tubular immaturity, observed during the first months of life, which is responsible for impaired sodium and water reabsorption. This may predispose to failure to thrive and dehydration under pathological circumstances (1). It has been suggested that alteration of sodium reabsorption during perinatal life could be

ISSN Print 0013-7227 ISSN Online 1945-7170
Printed in U.S.A.

doi: 10.1210/en.2008-1498 Received October 24, 2008. Accepted May 14, 2009.
First Published Online May 28, 2009

Abbreviations: AQP2, Aquaporin 2; CCD, cortical collecting duct; D0, postnatal d0; E18, embryonic d18; αENaC, α-subunit of the epithelial sodium channel; GR, glucocorticoid receptor; 11βHSD2, 11β-hydroxysteroid dehydrogenase type 2; mMR, murine MR, MR, mineralocorticoid receptor; qPCR, quantitative real-time PCR; V2R, arginine-vasopressin receptor.

related to a partial and transient tubular resistance to aldosterone (2). Indeed, high plasma levels of aldosterone have been described throughout the first year of life and reached normal adult values at 12 months of age (3). Numerous cases of transient pseudohypoaldosteronism have also been reported, all in neonates under 3 months of age who presented with dehydration associated with hyponatremia, hyperkalemia, and high plasma aldosterone and renin levels during an episode of pyelonephritis. Clinical symptoms and biological parameters normalized after resolution of the infection (4, 5). All these observations suggest a partial renal unresponsiveness to aldosterone in the newborn, whose pathogenesis has never been determined.

Most aldosterone effects are mediated by the mineralocorticoid receptor (MR), a transcription factor member of the nuclear receptor family (6). The human MR gene (*hMR*) is localized on chromosome 4 in the q31.1 region (7) and spans over approximately 450 kb (8). The gene is composed of 10 exons. The first two exons, 1α and 1β, are untranslated, and their alternative transcription gives rise to two splice variants: MRα and MRβ, expressed in various human tissues including the kidney (9). Importantly, both isoforms encode the same MR protein (6).

In the cortical collecting duct (CCD) cells, aldosterone, by binding to MR, regulates various genes implicated in sodium and water transport such as the α-subunit of the epithelial sodium channel (αENaC) (10), Na-K-ATPase (11), and aquaporin 2 (AQP2) (12). In epithelial cells, the enzyme 11β-hydroxysteroid dehydrogenase type 2 (11βHSD2) controls, at a prereceptor level, the selectivity of the aldosterone-MR signaling pathway by metabolizing cortisol into cortisone, which is unable to bind to MR (13, 14). Two other proteins expressed in CCD cells are important for sodium and water homeostasis: the glucocorticoid receptor (GR), which shares ligands, hormone-responsive elements, and molecular partners with MR (6), and the arginine-vasopressin receptor (V2R), which regulates AQP2 intracellular shuttling (15).

Very little is known about the sequential organization and regulation of these different markers of epithelial CCD cells during embryogenesis. Renal ontogenesis in mammals comprises the succession of three different embryonic structures, the pronephros, mesonephros, and metanephros (16). Only the latter will develop and form the adult kidney. In human and mouse, renal ontogenesis takes place during different periods of development. In the mouse, renal formation starts at 8 d postcoitum and is completed 7 d after birth (mouse gestation is 20–21 d long), whereas in human, kidney formation occurs during gestation between 3 and 36 wk (16).

We hypothesized that the partial and transient aldosterone resistance observed in neonates might be due to a late-onset or variable MR expression during renal development. No quantitative investigation of MR expression during the perinatal period has ever been published. Here, we report direct evidence for the activation of the renin-angiotensin-aldosterone system in newborn infants. We also performed a comprehensive analysis of mouse and human MR mRNA and protein expression during renal ontogenesis, using quantitative real-time PCR (qPCR) analysis and immunohistochemistry. In parallel, we have studied the expression of the different MR mRNA isoforms (MRα and MRβ) as well as other molecular determinants of the mineralocorticoid pathway (αENaC and 11βHSD2) and other important factors implicated in sodium and water transport (GR, V2R, and AQP2).

We provide first evidence that MR is expressed at extremely low levels in human and mouse kidneys during the perinatal period, notwithstanding high aldosterone levels. Such a finding is an important step toward a better understanding of the physiology of neonatal sodium and water handling and of the pathogenesis of aldosterone resistance in newborns.

Materials and Methods

Aldosterone and renin measurements

Aldosterone and renin were measured in surplus plasma of umbilical cords taken for diagnostic purposes of 48 full-term eutrophic newborns (24 females and 24 males) immediately after delivery. Informed and written consent was obtained from their mothers. Hormonal levels were assessed using RIA kits, the Aldo-Riact, (Cisbio International, Gif sur Yvette, France), and the Renin III generation (Cisbio).

Mouse and human renal samples

Wild-type mouse kidneys were collected at different developmental stages from 15 d of gestation to 15 d postnatal. For each animal, one kidney was snap-frozen in liquid nitrogen for qPCR analyses or Western blot, and the other one was fixed in buffered formol and embedded in paraffin for immunohistochemistry. Animal housing and experiments were conducted according to the French legislation.

Thirty-seven archival formol-fixed paraffin-embedded fetal, neonatal, and infantile kidneys were selected from the collections of several departments of pathology according to the French legislation (Table 1). Quality and integrity of human samples were verified by immunostaining with vimentin (as a control of appropriate formol fixation) and a low molecular weight cytokeratin (as a control of epithelial tubular cell integrity). The human adult kidney sample, used as a positive control, was obtained from the healthy part of a nephrectomy for cancer, with the patient's written consent, in adherence to the Declaration of Helsinki.

Snap-frozen kidney samples from 19 fetuses aged from 14–40 wk gestation, obtained from the Fetopathology Department of Robert Debré Hospital were used for qPCR (Table 1). All fetal samples were collected after parental informed and written

TABLE 1. Number of snap-frozen and paraffin-embedded human kidney samples obtained for different periods of development and relative quantification of MR, GR, and AQP2 immunodetection

	Age					
	10–14 GW	**15–25 GW**	**30–40 GW**	**0–6 months**	**7–10 months**	**11 months to 11 yr**
No. of human renal samples						
Gene expression	1	15	3	0	0	0
Immunohistochemistry	2	7	5	5	7	11
MR immunostaining	0	+	0	0	0	++
GR immunostaining	+	++	+++	+	+	+++
AQP2 immunostaining	0	+++	+++	+++	+++	+++

Snap-frozen and paraffin-embedded samples were used for qPCR and immunohistochemistry, respectively. Fetal kidney samples originate from *in utero* fetal deaths with rapid delivery and autopsy within 24–36 h postmortem. Neonatal kidney samples (0–11 months) are from sudden infant deaths. Infantile kidney samples (11 months to 11 yr) come from the healthy part of nephrectomies for nephroblastoma. Although not directly quantitative, the evaluation of the staining was scored by both the number of immunolabeled cells and the labeling intensity within specific target structures. At least six × 20 power fields of renal cortex were studied for each immunolabeled section, each marker being studied at least on three nonconsecutive sections of each sample. An immunostaining score was attributed as follows: 0, below detection threshold; +, fewer than 10 weakly immunolabeled cells per field; ++, 10–50 moderately immunostained cells per field; +++, more than 50 strongly stained cells per field. GW, Gestational weeks.

consent and after declaration to the French Biomedical Agency (Decree 003812, 09/22/2006).

Primary antibodies

Four different antibodies were used: monoclonal anti-MR clone 6G1, generously provided by Dr. Gomez-Sanchez (University of Mississippi, MS) (17), polyclonal antimouse GR (Santa Cruz Biotechnology, Inc., Santa Cruz, CA), monoclonal antihuman GR (AbCys SA, Paris, France), and monoclonal anti-AQP2 (Santa Cruz) (18). Dilutions used were 1:120, 1:400, 1:10, and 1:1000, respectively. Monoclonal anti-vimentin clone V9 (Biogenex Laboratories, San Ramon, CA) and anti-keratin 19 antibodies (Progen, Queensland, Australia) were used at 1:120 dilution. For MR Western blot analysis, rabbit polyclonal anti-MR antibody (39N) was generated using the human MR 1–18 peptide and purified by affinity chromatography (Double X/XP boosting antibody production program; Eurogentec, Seraing, Belgium).

Immunohistochemistry

Five-micrometer-thick tissue sections were deparaffinized and rehydrated in successive baths of toluene and graded alcohols and subjected to 15 min microwave antigen retrieval in citrate buffer (pH 6.0) [Tris-EDTA buffer (pH 9) for the antihuman GR]. After cooling and 15 min preincubation with a blocking serum (Vector Laboratories, Burlingame, CA), slides were incubated with primary antibodies overnight at 4 C in a humid chamber. Bound Ig were revealed with the appropriate ImmPRESS antimouse or antirabbit Ig kit (Vector) according to the manufacturer's instructions.

Histological studies

The histological quality of the tissues and the stage of renal development were assessed by hematoxylin-eosin staining.

Quantitative real-time RT-PCR

Two micrograms of total RNA, isolated from frozen samples, were subjected to deoxyribonuclease I treatment (Invitrogen) and reverse-transcribed with 200 U reverse transcriptase (Superscript II; Invitrogen). PCR were performed with 100 ng cDNA in the presence of qPCR Mastermix Plus for Sybr Green I (Eurogentec) containing 300 nM specific primers (supplemental Tables 1 and 2, published as supplemental data on The Endocrine Society's Journals Online web site at http://endo.endojournals.org). qPCR was carried on an ABI 7300 Sequence Detector (Applied Biosystems, Foster City, CA). For standards preparation, amplicons were subcloned into pGEMT-Easy plasmid (Promega, Madison, WI) and sequenced to confirm the identity of each sequence. Standards for different MR isoforms were determined by use of specific primers designed in exons 2 and 3 for the MR, exons 1α and 2 for MRα, and exons 1β and 2 for MRβ. Standard curves were generated using serial dilutions of linearized standard plasmids. Samples were amplified in duplicate or triplicate. Ribosomal 18S was used as an internal control for data normalization. Relative expression of a given gene is expressed as the ratio attomoles of specific gene per femtomole of 18S.

Western blot analyses

Total protein extracts were prepared from a pool of frozen murine kidneys at various developmental stages [embryonic d 18 (E18), postnatal d 0 (D0), D8, and adult]. Briefly, frozen kidneys were ground in a mortar under liquid nitrogen, and lysis buffer [25 mM Tris-HCl (pH 7.5), 150 mM NaCl, 5 mM EDTA, 30 mM Na pyrophosphate, 50 mM Na fluoride, 0.1% Triton X-100, 1× protease inhibitor cocktail (Sigma Chemical Co., St. Louis, MO)] was added to the resulting powder. Homogenates were obtained with a Teflon glass potter at 4 C and centrifuged at 13,000 rpm at 4 C for 20 min. Aliquots of supernatant were frozen in liquid nitrogen until further use. Immunoblots were incubated overnight in 5% milk/Tris-buffered saline/0.1% Tween 20 followed by incubation for 1 h at room temperature with affinity purified anti-MR 39N (1:2000) and with peroxidase-conjugated goat antirabbit antibody, dilution 1:15,000 (Vector) and visualized by the ECL$^+$ detection kit. For loading normalization, membranes were incubated with anti-α-tubulin antibody (Sigma). Quantitative analysis of specific signals was performed using Quantity One software (Bio-Rad, Marnes-la-Coquette, France).

Statistical analyses

Results represent mean ± SEM for the mouse samples with at least six samples for each developmental stage. For human samples, results are expressed as the mean of at least three indepen-

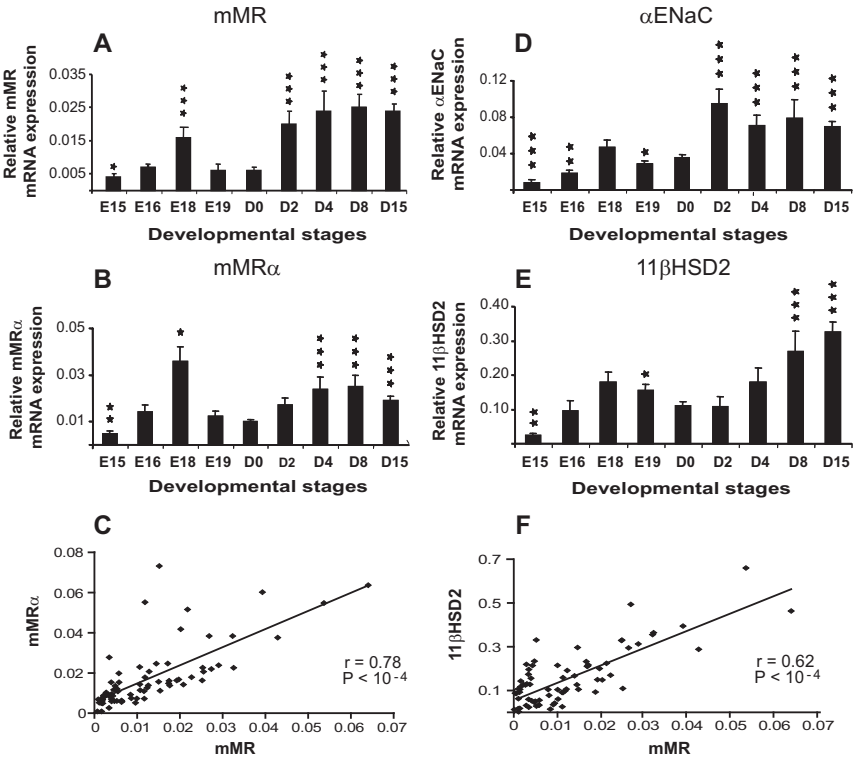

FIG. 1. Ontogenesis of mMR, mMRα, αENaC, and 11βHSD2 mRNA expression during mouse kidney development. A, B, D, and E, Relative mRNA expression levels were determined using qPCR at various developmental stages as follows: E15–19, D0, and D2–D15. D0 was used as reference for statistical analysis: *, $P < 0.05$; **, $P < 0.01$; ***, $P < 0.001$. Results, expressed as the ratio of attomoles of specific gene per femtomole 18S, are mean ± SEM (E15 n = 6, E16 n = 8, E18 n = 10, E19 n = 12, D0 n = 15, D2 n = 6, D4 n = 6, D8 n = 6, and D15 n = 6). C and F, Correlations between the relative expression of mMR *vs.* mMRα (C) or 11βHSD2 (F) were obtained by Spearman regression analysis.

dent analyses of three different reverse-transcribed samples. Statistical analyses were performed using a nonparametric Mann Whitney *U* test (Prism4; GraphPad Software, Inc., San Diego, CA). Correlations between two parameters were obtained by Spearman regression analysis, with significant threshold at 0.05.

Results

Activation of the renin-angiotensin-aldosterone system at birth

High levels of aldosterone and renin levels were observed in umbilical cord blood of 48 healthy newborns [mean and median of 817.1 and 662.5 pg/ml (range 105–2211) and 78.8 and 50.0 pg/ml (range 12–288), respectively), statistically different ($P < 0.001$) from normal plasma aldosterone and renin concentration values in healthy adults (n = 50), which were 99 ± 43 and 8.1 ± 3.7 pg/ml, respectively.

Expression of MR and its signaling partners during mouse renal development

Quantitative mRNA expression

Murine MR (mMR) mRNA expression was quantified by qPCR at various developmental stages between E15 and D15 (Fig. 1A) and compared with the day of birth (D0) chosen as the statistical reference. At E15, mMR transcript is hardly detectable. Its expression begins to increase significantly at E16 and reaches a maximum (4-fold increase) at E18 (relative expression 0.016 amol/fmol 18S). During the period surrounding birth (E19 and D0), mMR mRNA expression is surprisingly low, with levels comparable to E16 (0.004 amol/fmol). Thereafter, it increases again progressively until D15.

We next examined the relative expression of mMRα and mMRβ isoforms, using specific primers. We found a similar expression profile for mMRα isoform (Fig. 1B), with an onset of expression at E16, a 2.5-fold increase at E18, and a significant decrease at E19 and D0. A high positive correlation between mMR and mMRα isoform expression profiles is found (Fig. 1C). Similar results are obtained with the mMRβ isoform (data not shown).

To investigate whether other genes of the mineralocorticoid signaling pathway had the same evolution profile, we quantified αENaC and 11βHSD2 mRNA throughout development. Like mMR, their renal expression increases from E16 to E18 and is down-regulated at E19 and D0 before increasing again after birth (Fig. 1, D and E). There is a highly significant correlation between mMR and the expression profiles of 11βHSD2 (Fig. 1F) and αENaC (data not shown), suggesting a comparable maturation process for different markers of the late distal nephron.

We also analyzed GR, V2R, and AQP2 gene expression during renal development (supplemental Fig. 1). At variance with mMR, renal GR expression has a very different profile. GR mRNA is already present at E15, increases slightly at E16, but does not vary significantly at other developmental stages. Like MR, V2R and AQP2 transcripts are first detected at E16 as previously described (19, 20). In contrast, unlike MR, V2R, and AQP2 expression increases progressively until D15, with no nadir at birth.

MR, GR, and AQP2 protein expression

Immunohistochemical studies, using a monoclonal antibody directed against the MR first 18 amino acids (17) revealed that the MR protein seems to be mostly detected in the nuclei of the CCD cells at all developmental stages

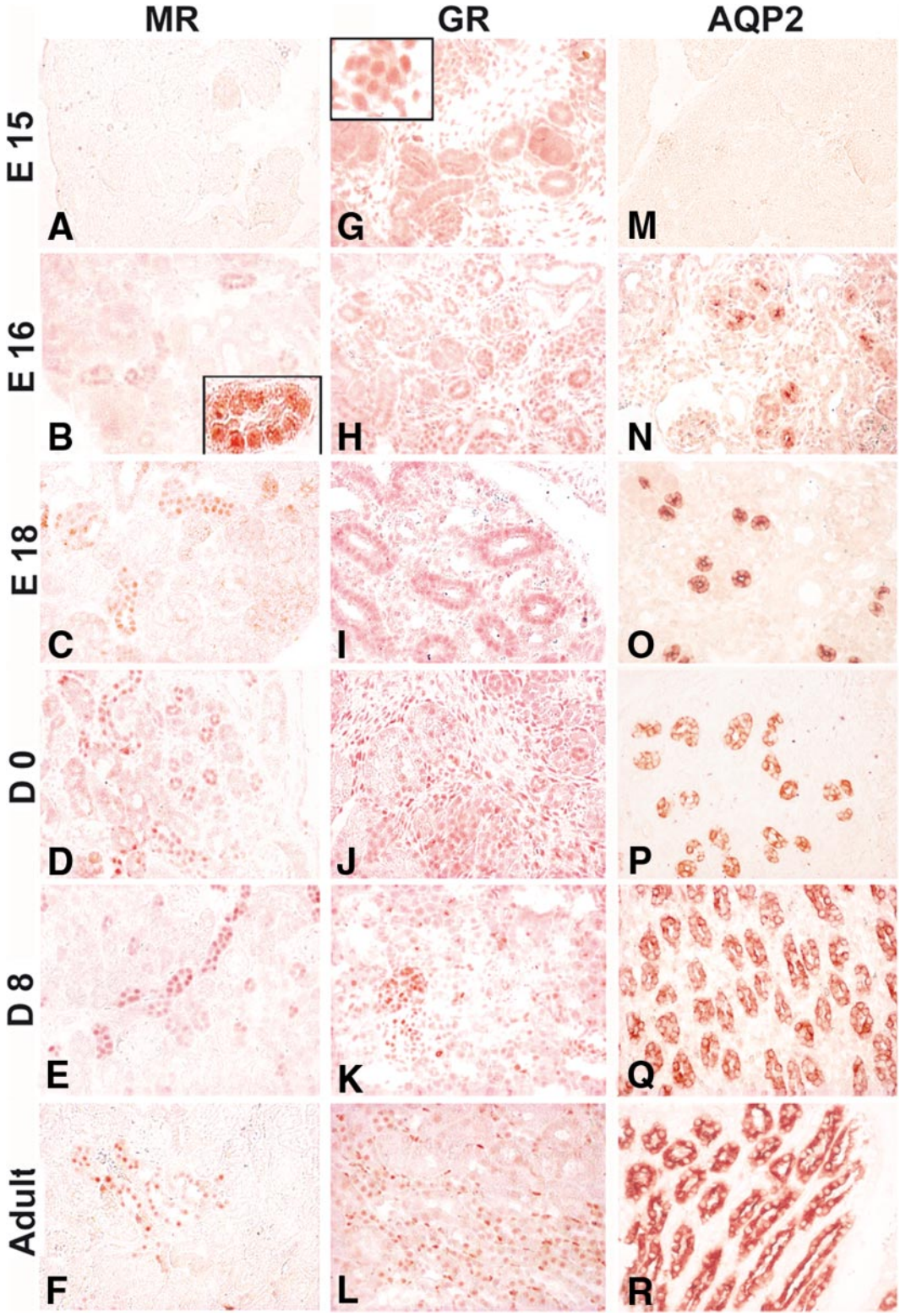

FIG. 2. Immunodetection of MR, GR, and AQP2 during renal development of murine fetus and neonates. A–F, Immunoreactive MR protein is absent at E15 (A) but begins to be detected at E16, most notably in the nuclei of CCD cells (B, see *inset*; see also supplemental Fig. 2). MR expression is rather weak at E18 and D0 but increases afterward at D8 and in the adult kidney. G–L, GR protein is already present at E15 (G) in the nuclei (see *inset*) of endothelial, interstitial, and epithelial cells in different segments of the nephron and in the glomeruli (H–L). M–R, A strong AQP2 immunostaining is observed at the apical membrane of the CCD cells from E16 to adulthood (N–R). Original magnification, × 20; *insets*, × 100.

from E16 to D15 and in adult kidney (Fig. 2, B–F, and supplemental Fig. 2). No staining is observed at E15 (Fig. 2A). At E16, MR immunodetection is faint and increases throughout the developmental stages studied, with an extension to additional CCD cells. Importantly, MR is never detected in the glomeruli, in the proximal convoluted tubule, in the arteries, or in the interstitial cells. On the contrary, GR protein, which is already present at E15, is detected not only in the nuclei of the CCD cells (Fig. 2G) but also in the glomeruli, in different segments of the nephron (proximal and distal convoluted tubules, Henle's loop), and in endothelial and interstitial cells (Fig. 2, G–L). The AQP2 protein is first expressed at E16. In contrast to the weak MR expression, strong cytoplasmic immunostaining, particularly at the apical membrane of the CCD cells is observed until D15 (Fig. 2, M–R). These findings corroborate our qPCR results, because both AQP2 transcript and protein appear initially on E16.

Western blot analysis of kidneys obtained from murine fetal, postnatal, and adult animals at different developmental stages showed an extremely low level of MR expression in the kidneys of E18 as well as D0 mice. In sharp contrast, the renal MR expression was dramatically upregulated at D8, reaching adult values (Fig. 3). These data fully confirm that in the mouse, renal MR, at both the mRNA and protein level, is very low at birth.

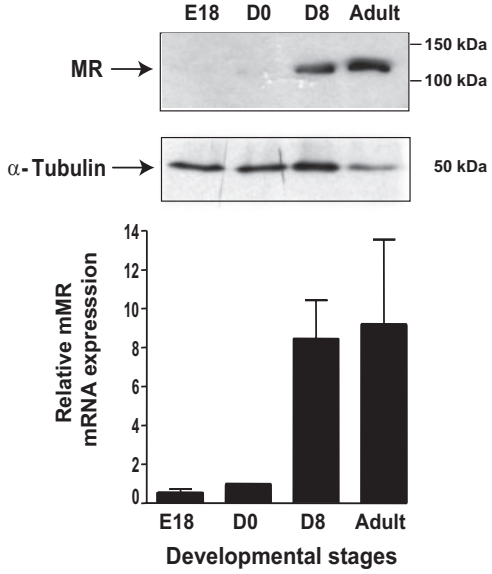

FIG. 3. Western blot analysis of MR expression during murine renal development. Twenty micrograms of protein from kidney homogenates at different developmental stages (E18, D0, D8, and adult) were loaded on 7.5% SDS-PAGE followed by direct immunoblotting with anti-MR 39N antibody (1/2000). α-Tubulin was used as loading control. MR was normalized to α-tubulin protein levels after digitalization on a gel scanner using Quantity One software (Bio-Rad). Results are means ± SD of four independent determinations and are expressed relative to MR expression measured at D0, arbitrarily set at 1.

Expression of hMR and its signaling partners during human renal development

Quantitative mRNA expression

Nineteen human fetal renal samples (14–40 wk) (see Table 1) were used to quantify hMR mRNA expression by qPCR (Fig. 4A). Relative hMR expression is lowest at 14 wk, increases at 16 wk, and peaks at 19 wk. Renal hMR mRNA levels decrease afterward, around 25 wk gestation. The expression of both hMRα and hMRβ isoforms is highly correlated with hMR expression (supplemental Fig. 3). αENaC and 11βHSD2 transcripts are expressed in human kidney and share the same evolution profile as hMR isoforms. The best correlation scores are found for hMRα and αENaC (Fig. 4B) and hMRα and 11βHSD2 (Fig. 4C).

We also quantified the relative expression of GR, V2R, and AQP2 (supplemental Fig. 4). GR transcript level is stable during gestation. On the contrary, V2R mRNA expression is relatively low, whereas AQP2, whose maximal

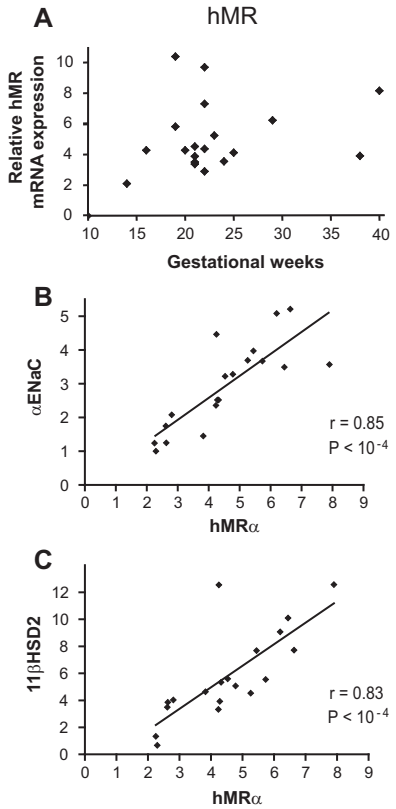

FIG. 4. Ontogenesis of hMR mRNA expression during human kidney development. A, Relative hMR expression was determined using qPCR in fetal kidney samples at various gestational ages. Each point represents the mean of three independent determinations of hMR expression, performed in triplicate in a given sample (see *Materials and Methods*), and normalized by hMR expression in one adult kidney sample (0.04 ± 0.008 amol/pmol 18S, mean ± SEM; n = 11). B and C, Correlations between the expression of hMRα isoform *vs.* αENaC (B) or 11βHSD2 (C) were obtained by Spearman regression analysis.

values are reached later during renal maturation (24 wk), is highly expressed during development.

MR, GR, and AQP2 protein expression during human kidney development

A collection of 37 paraffin-embedded human kidney samples from 14 fetuses, 12 neonates (0–11 months old), and 11 children (1–11 yr old) was used to analyze and quantify MR, GR, and AQP2 protein expression during fetal and postnatal renal development (Table 1 and Figs. 5 and 6). The integrity of all samples was assessed by a hematoxylin-eosin staining, which allowed assessing the stages of kidney development (Figs. 5, A–D, and 6, A–C). As expected, we observed that formation of glomeruli and nephrons and the architectural organization of the kidney take place between 5 and 36 wk gestation. We noticed that, at higher magnification, podocytes in several glomeruli still retain an immature cubic shape around 40 wk of gestation (Fig. 5D), whereas their mature flattened shape is observed in every glomerulus only at approximately 1 yr of age (Fig. 6B). This confirms that some nephrons achieve functional maturity only during the postnatal period, according with previous studies (21). Tissue integrity was verified using two specific antibodies

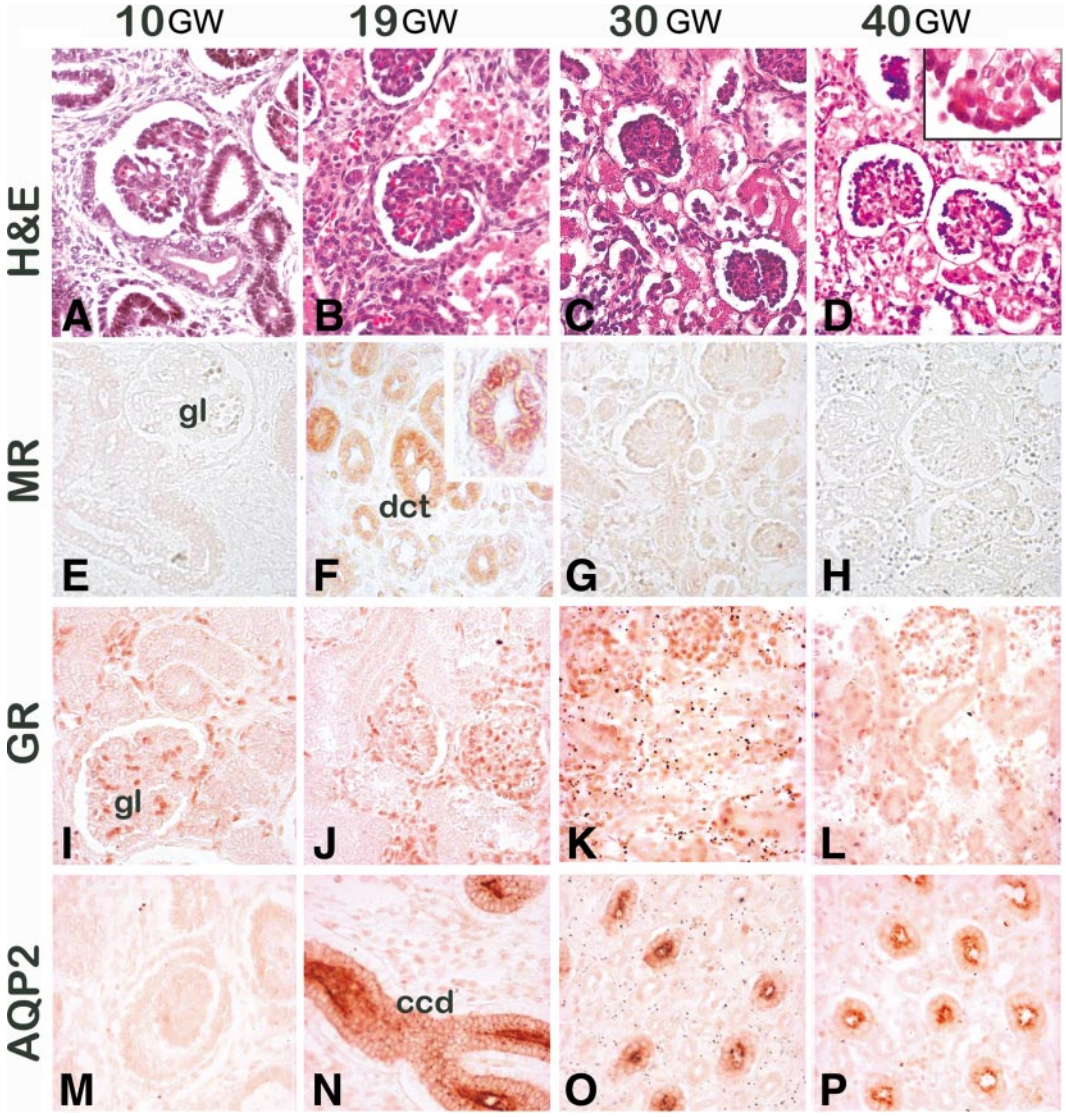

FIG. 5. Histology and MR, GR, and AQP2 immunoreactivity in human fetal kidneys. A–D, Hematoxylin and eosin (H&E) staining at various stages of fetal renal development. At 10 gestational weeks (GW), the human kidney is clearly immature (A). At 40 GW (D), glomeruli and nephron formation is achieved, but some podocytes preserve an immature cubic shape (*inset*, D). E–H, MR immunodetection is observed at specific stages of renal development. Immunoreactive MR is transiently detected in distal collecting ducts at 19 GW, as illustrated by a positive staining, mostly in the nuclear compartment (*inset*, F). In contrast, no renal MR expression is found at 10 GW (E) and from 30–40 GW (G and H). I–L, The GR protein is immunodetected at all developmental stages in the nuclei of endothelial, interstitial, and epithelial cells in different nephronic segments and the glomeruli. M–P, AQP2 is not expressed at 10 GW (M), whereas a strong immunostaining is detected at the apical membrane of the CCD cells from 15–40 GW (N, O, and P). Original magnification, × 20; *insets*, × 100. dct, Distal convoluted tubule; gl, glomerulus.

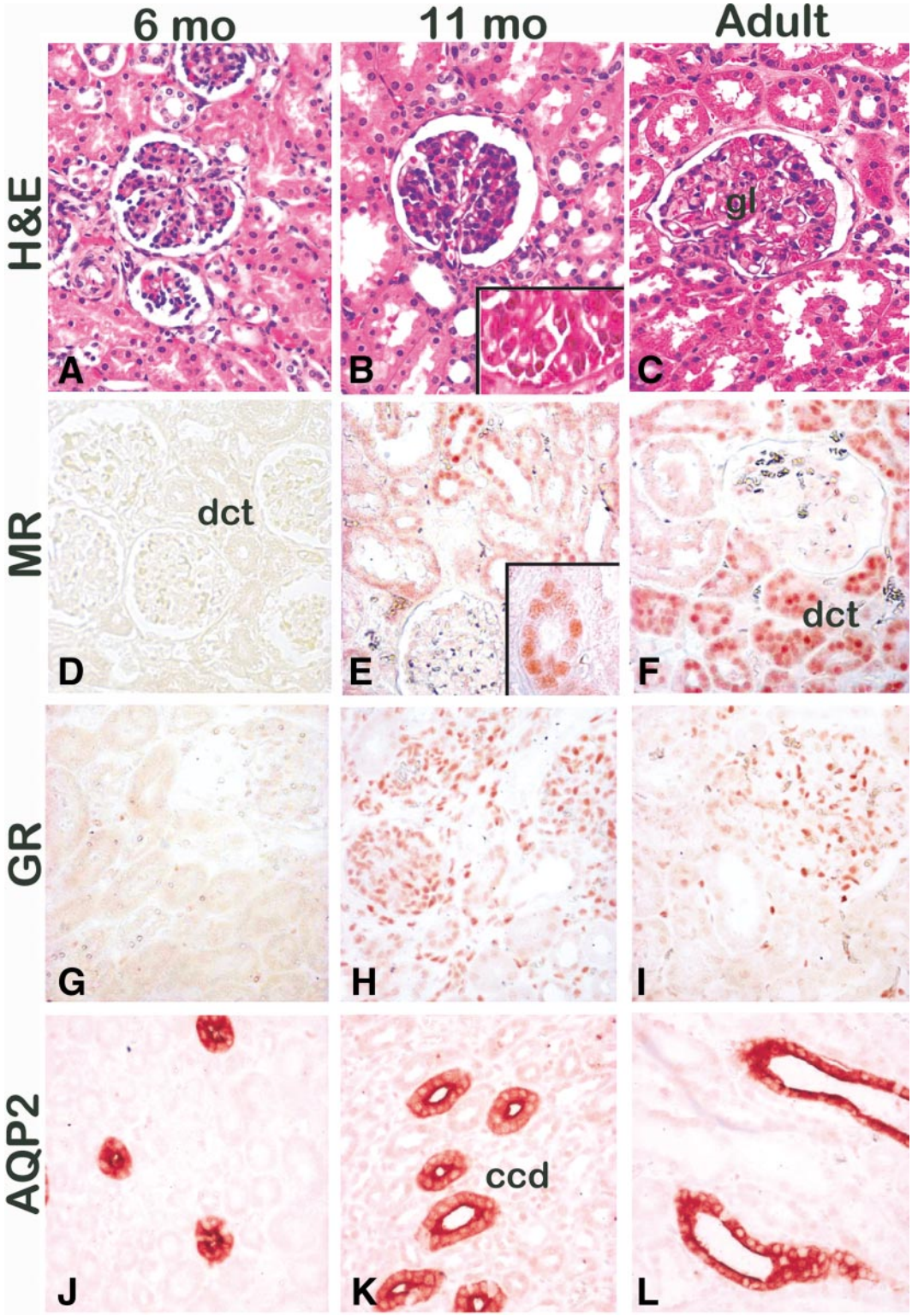

FIG. 6. Histology and MR, GR, and AQP2 immunoreactivity in human neonatal and adult kidneys. A–C, Hematoxylin and eosin (H&E) staining at various stages of postnatal renal development. Podocytes have reached a mature flattened shape at 11 months postnatal (*inset*, B). D–F, MR immunodetection is observed at specific stages of postnatal renal development. No MR protein is detected from birth until 11 postnatal months (D). Afterward, MR immunoreactivity is readily detected at 11 months after birth (E) as in the adult kidney (F). G–I, GR is weakly expressed during the 2- to 10-month postnatal period (G). Afterward, GR protein is strongly expressed in the nuclei of endothelial, interstitial, and epithelial cells in different parts of the nephron and the glomeruli (H and I). J–L, A strong AQP2 immunostaining is detected at the apical membrane of the CCD cells from birth to adulthood. Original magnification, × 20. dct, Distal convoluted tubule; gl, glomerulus.

recognizing well-characterized markers of CCD cells (cytokeratin 19) (22) and mesenchymal cells (vimentin) (23).

Using the same MR-specific monoclonal antibody (17), MR protein was immunodetected at 15 wk gestation, mostly in the nuclei of the CCD cells (Fig. 5F). MR is absent in 10-wk-old samples (Fig. 5E). The immunoreactivity is present in all seven samples from 15–24 wk gestation (Fig. 5F). Interestingly, no MR is observed perinatally in human kidneys. The immunostaining is negative in all 17 samples from 30 wk gestation to 10 months of age (Figs. 5, G and H, and 6D). MR expression is again observed at 11 months after birth and is present in all the 11 samples studied, from 11 months to 11 yr (Fig. 6E). The intensity of the immunostaining and the number of immunopositive cells in the CCD increase throughout postnatal development.

GR expression is detected earlier than MR, starting from 10 wk gestation. The labeling is nuclear and localized in the nuclei of not only the tubular epithelial cells but also in the glomerular, endothelial, and interstitial cells (Fig. 5I). The GR protein is present at all stages of fetal development (Fig. 5, I–L) and during the first 2 months after birth. Afterward, between 2 and 10 months, the immunoexpression is variable, with five samples of 11 being immunonegative or weakly positive (Fig. 6G). However, after 11 months, the GR protein is consistently found in all samples (Fig. 6H). These results suggest an early functional role for GR during human embryogenesis and, like MR, a variability of expression during specific periods of development.

AQP2 is first detected at 15 wk gestation, localized at the membrane of CCD epithelial cells with accentuation at the apical pole (Fig. 5N). Unlike MR, the staining intensity is constantly strong, and the immunolabeling is present at all renal developmental stages from 15 wk gestation to 11 yr after birth and in the adult kidney (Figs. 5, N–P, and 6, J–L).

Taken together, these results indicate that, as for the mouse, MR has a biphasic expression during human renal development, with a transient expression during gestation that seems to be restricted to the mineralocorticoid signaling pathway. Thus, the low renal MR expression during the early postnatal period might account for the transient aldosterone resistance observed in newborns.

Discussion

Kidney growth and differentiation during embryonic and fetal development is a complex process in which the maturation of the distal nephron is directly correlated with the renal capacity to regulate sodium and water transport. Herein, we demonstrate that different key players of the mineralocorticoid signaling pathway (11βHSD2, MR isoforms, and αENaC), involved in the control of renal sodium reabsorption (24), have a parallel temporal evolution during renal ontogenesis. Their expression in the kidney peaks at E18 in the mouse and between 19 and 24 wk in the human fetus. These results are in accordance with previous *in situ* hybridization studies that found the onset of MR mRNA expression in the murine kidney at 18 d postcoitum (25) and demonstrated the presence of MR transcripts between 6 and 16 wk (26) and of immunoreactive MR protein between 14 and 20 wk human gestation (27). However, no quantitative analysis of MR expression in the perinatal period has ever been reported, considering the difficulty of collecting such samples. In the present study, we provide the first evidence for a transient renal MR expression during both murine and human fetal life, which seems to coincide with skin keratinization, a very specific stage of fetal development. Indeed, before 20 wk human gestation and 17 d postcoitum in the mouse, the absence of a physiological impermeable barrier facilitates the free exchange between fetal extracellular fluid and amniotic fluid (28, 29). In contrast, after full keratinization, the maintenance of sodium balance becomes a highly regulated and dynamic process prominently regulated by renal MR. The decline in renal MR expression after 24 wk (human) and 18 d (mouse) of conception could be explained by modifications in the sodium concentration of the amniotic fluid (30), whose resorption by fetal swallowing constitutes a major mechanism regulating sodium intake. This is reminiscent of variation in MR expression observed in salmons during their acclimation from fresh to salt water (31). In any case, this transient expression seems dispensable for fetal kidney development because pseudohypoaldosteronism type 1 (PHA1a) patients, presenting with heterozygous MR-inactivating mutations (32), and MR knockout newborn mice (33) exhibit normal renal morphology (34).

Interestingly, high aldosterone levels in human umbilical cords are associated with an extremely low or undetectable renal MR expression at birth. The molecular mechanisms underlying MR expression are very complex, involving the use of alternative tissue-specific promoters (35, 36). The profound hormonal changes associated with labor and delivery are likely to be involved in MR downregulation. Whether changes in MR expression are a direct consequence of fetal acclimation from an aquatic (intrauterine) environment to extrauterine terrestrial life remains to be elucidated.

The critical role played by MR on sodium balance during the postnatal period is now well established. Indeed, MR knockout mice die shortly after birth, around d 8, of dehydration and failure to thrive (33), and children with PHA1a present with salt wasting ascribed to MR haploinsufficiency (32). Both phenotypes are rescued by sodium supplementation (32, 37). In healthy newborns, the ab-

sence of dehydration or failure to thrive indicates that renal MR levels are sufficient to ensure appropriate sodium balance, even though MR expression was below our immunodetection limit in the perinatal period. In sharp contrast, preterms have constant salt loss and an impaired capacity to concentrate urine, causing a major problem to pediatricians (1). Given the presence of AQP2 at both the mRNA and protein level, this renal phenotype could be partly explained by very low levels of MR, known to be involved in AQP2 cellular trafficking and protein up-regulation (12, 38).

In mice and humans, renal MR levels progressively increase after birth, after renal maturation, which is achieved by D8 in rodents and approximately 1 yr after birth in humans (1). Our findings indicate that MR expression in the postnatal period parallels the full maturation of the late distal nephron. The regulatory mechanisms governing MR expression are currently unknown, but it is likely that the dynamic setting of a functional MR signaling predicts the physiological adaptation of the neonate to its new environment.

In conclusion, we provide the first evidence both in mouse and human of a biphasic temporal expression of MR and of other partners of the mineralocorticoid signaling pathway during renal development. There is a major but transient peak of MR expression during fetal life, concomitant with fetal skin keratinization, whereas the progressive increase after birth correlates with full renal maturation. Our results also indicate that the low MR expression at birth could constitute the molecular basis of the partial aldosterone resistance during the neonatal period. Further experiments are required to evaluate whether similar expression profiles are detected in other aldosterone target tissues. Elucidation of mechanisms regulating MR levels could ultimately lead to new therapeutic strategies for the management of sodium loss in preterms and neonates and, possibly, of renal (39–41) and heart diseases (39, 42) in adulthood.

Acknowledgments

We thank Prof. Stephane Droupy (Department of Urology, Bicêtre Hospital, France) for his help and to Prof. Michael Freemark (Duke University Medical Center, Durham, NC) for carefully reading this manuscript. The assistance of Annick Ganieux and Nathalie Ba (IFR 93, Bicêtre, France) is also gratefully acknowledged.

Address all correspondence and requests for reprints to: Dr. Marc Lombes, M.D., Ph.D., Inserm U693, Faculté de Médecine Paris-Sud, 63, rue Gabriel Péri, 94276 Le Kremlin Bicêtre Cedex, France. E-mail: marc.lombes@u-psud.fr.

Disclosure Summary: L.M., S.V., A.-L.D., F.J., M.S., S.P., P.B., and G.M. have nothing to disclose. M.L. received a research grant from Pfizer Laboratories (2008–2009).

This work was supported by funds from Institut National de la Santé et de la Recherche, University Paris-Sud 11 and the European Section of Aldosterone Council. Fellowships (to L.M.) were from the Association des Juniors en Pédiatrie, the Société Française d'Endocrinologie et Diabétologie Pédiatrique, Gallia and Pfizer Laboratories, France, and the Fonds d'Etudes et de Recherche du Corps Médical des hôpitaux de Paris.

References

1. **Holtbäck U, Aperia AC** 2003 Molecular determinants of sodium and water balance during early human development. Semin Neonatol 8:291–299
2. **Aperia A, Broberger O, Herin P, Zetterström R** 1979 Sodium excretion in relation to sodium intake and aldosterone excretion in newborn pre-term and full-term infants. Acta Paediatr Scand 68:813–817
3. **Mehta KP, Karnik SR, Sathe A, Pant R, Khatwani R, Bhise A** 1992 Renal parameters during infancy. Indian Pediatr 29:1385–1390
4. **Dolezel Z, Starha J, Novotna D, Dostalkova D** 2004 Secondary pseudohypoaldosteronism in an infant with pyelonephritis. Bratisl Lek Listy 105:435–437
5. **Maruyama K, Watanabe H, Onigata K** 2002 Reversible secondary pseudohypoaldosteronism due to pyelonephritis. Pediatr Nephrol 17:1069–1070
6. **Viengchareun S, Le Menuet D, Martinerie L, Munier M, Pascual-Le Tallec L, Lombès M** 2007 The mineralocorticoid receptor: insights in its molecular and (patho)physiological biology. Nucl Recept Signal 5:e012
7. **Morrison N, Harrap SB, Arriza JL, Boyd E, Connor JM** 1990 Regional chromosomal assignment of the human mineralocorticoid receptor gene to 4q31.1. Hum Genet 85:130–132
8. **Zennaro MC, Keightley MC, Kotelevtsev Y, Conway GS, Soubrier F, Fuller PJ** 1995 Human mineralocorticoid receptor genomic structure and identification of expressed isoforms. J Biol Chem 270: 21016–21020
9. **Zennaro MC, Farman N, Bonvalet JP, Lombès M** 1997 Tissue-specific expression of α and β messenger ribonucleic acid isoforms of the human mineralocorticoid receptor in normal and pathological states. J Clin Endocrinol Metab 82:1345–1352
10. **Mick VE, Itani OA, Loftus RW, Husted RF, Schmidt TJ, Thomas CP** 2001 The α-subunit of the epithelial sodium channel is an aldosterone-induced transcript in mammalian collecting ducts, and this transcriptional response is mediated via distinct *cis*-elements in the 5′-flanking region of the gene. Mol Endocrinol 15:575–588
11. **Derfoul A, Robertson NM, Lingrel JB, Hall DJ, Litwack G** 1998 Regulation of the human Na/K-ATPase β1 gene promoter by mineralocorticoid and glucocorticoid receptors. J Biol Chem 273:20702–20711
12. **Hasler U, Mordasini D, Bianchi M, Vandewalle A, Féraille E, Martin PY** 2003 Dual influence of aldosterone on AQP2 expression in cultured renal collecting duct principal cells. J Biol Chem 278:21639–21648
13. **Edwards CR, Stewart PM, Burt D, Brett L, McIntyre MA, Sutanto WS, de Kloet ER, Monder C** 1988 Localisation of 11β-hydroxysteroid dehydrogenase: tissue specific protector of the mineralocorticoid receptor. Lancet 2:986–989
14. **Funder JW, Pearce PT, Smith R, Smith AI** 1988 Mineralocorticoid action: target tissue specificity is enzyme, not receptor, mediated. Science 242:583–585
15. **Hayashi M, Sasaki S, Tsuganezawa H, Monkawa T, Kitajima W, Konishi K, Fushimi K, Marumo F, Saruta T** 1996 Role of vasopressin V2 receptor in acute regulation of aquaporin-2. Kidney Blood Press Res 19:32–37

16. **Kuure S, Vuolteenaho R, Vainio S** 2000 Kidney morphogenesis: cellular and molecular regulation. Mech Dev 92:31–45
17. **Gomez-Sanchez CE, de Rodriguez AF, Romero DG, Estess J, Warden MP, Gomez-Sanchez MT, Gomez-Sanchez EP** 2006 Development of a panel of monoclonal antibodies against the mineralocorticoid receptor. Endocrinology 147:1343–1348
18. **Fischer E, Legue E, Doyen A, Nato F, Nicolas JF, Torres V, Yaniv M, Pontoglio M** 2006 Defective planar cell polarity in polycystic kidney disease. Nat Genet 38:21–23
19. **Ostrowski NL, Young 3rd WS, Knepper MA, Lolait SJ** 1993 Expression of vasopressin V1a and V2 receptor messenger ribonucleic acid in the liver and kidney of embryonic, developing, and adult rats. Endocrinology 133:1849–1859
20. **Yamamoto T, Sasaki S, Fushimi K, Ishibashi K, Yaoita E, Kawasaki K, Fujinaka H, Marumo F, Kihara I** 1997 Expression of AQP family in rat kidneys during development and maturation. Am J Physiol 272:F198–F204
21. **Thony HC, Luethy CM, Zimmermann A, Laux-End R, Oetliker OH, Bianchetti MG** 1995 Histological features of glomerular immaturity in infants and small children with normal or altered tubular function. Eur J Pediatr 154:S65–68
22. **Moll R, Franke WW, Schiller DL, Geiger B, Krepler R** 1982 The catalog of human cytokeratins: patterns of expression in normal epithelia, tumors and cultured cells. Cell 31:11–24
23. **Battifora H** 1991 Assessment of antigen damage in immunohistochemistry. The vimentin internal control. Am J Clin Pathol 96:669–671
24. **Booth RE, Johnson JP, Stockand JD** 2002 Aldosterone. Adv Physiol Educ 26:8–20
25. **Brown RW, Diaz R, Robson AC, Kotelevtsev YV, Mullins JJ, Kaufman MH, Seckl JR** 1996 The ontogeny of 11β-hydroxysteroid dehydrogenase type 2 and mineralocorticoid receptor gene expression reveal intricate control of glucocorticoid action in development. Endocrinology 137:794–797
26. **Condon J, Gosden C, Gardener D, Nickson P, Hewison M, Howie AJ, Stewart PM** 1998 Expression of type 2 11β-hydroxysteroid dehydrogenase and corticosteroid hormone receptors in early human fetal life. J Clin Endocrinol Metab 83:4490–4497
27. **Hirasawa G, Sasano H, Suzuki T, Takeyama J, Muramatu Y, Fukushima K, Hiwatashi N, Toyota T, Nagura H, Krozowski ZS** 1999 11β-Hydroxysteroid dehydrogenase type 2 and mineralocorticoid receptor in human fetal development. J Clin Endocrinol Metab 84:1453–1458
28. **Modena AB, Fieni S** 2004 Amniotic fluid dynamics. Acta Biomed 75(Suppl 1):11–13
29. **Ouellet T, Lussier M, Babaï F, Lapointe L, Royal A** 1990 Differential expression of the epidermal K1 and K10 keratin genes during mouse embryo development. Biochem Cell Biol 68:448–453
30. **Cheung CY, Brace RA** 2005 Amniotic fluid volume and composition in mouse pregnancy. J Soc Gynecol Investig 12:558–562
31. **Kiilerich P, Kristiansen K, Madsen SS** 2007 Hormone receptors in gills of smolting Atlantic salmon, Salmo salar: expression of growth hormone, prolactin, mineralocorticoid and glucocorticoid receptors and 11β-hydroxysteroid dehydrogenase type 2. Gen Comp Endocrinol 152:295–303
32. **Geller DS, Zhang J, Zennaro MC, Vallo-Boado A, Rodriguez-Soriano J, Furu L, Haws R, Metzger D, Botelho B, Karaviti L, Haqq AM, Corey H, Janssens S, Corvol P, Lifton RP** 2006 Autosomal dominant pseudohypoaldosteronism type 1: mechanisms, evidence for neonatal lethality, and phenotypic expression in adults. J Am Soc Nephrol 17:1429–1436
33. **Berger S, Bleich M, Schmid W, Cole TJ, Peters J, Watanabe H, Kriz W, Warth R, Greger R, Schütz G** 1998 Mineralocorticoid receptor knockout mice: pathophysiology of Na^+ metabolism. Proc Natl Acad Sci USA 95:9424–9429
34. **Hubert C, Gasc JM, Berger S, Schütz G, Corvol P** 1999 Effects of mineralocorticoid receptor gene disruption on the components of the renin-angiotensin system in 8-day-old mice. Mol Endocrinol 13:297–306
35. **Zennaro MC, Le Menuet D, Lombès M** 1996 Characterization of the human mineralocorticoid receptor gene 5′-regulatory region: evidence for differential hormonal regulation of two alternative promoters via nonclassical mechanisms. Mol Endocrinol 10:1549–1560
36. **Le Menuet D, Viengchareun S, Penfornis P, Walker F, Zennaro MC, Lombès M** 2000 Targeted oncogenesis reveals a distinct tissue-specific utilization of alternative promoters of the human mineralocorticoid receptor gene in transgenic mice. J Biol Chem 275:7878–7886
37. **Bleich M, Warth R, Schmidt-Hieber M, Schulz-Baldes A, Hasselblatt P, Fisch D, Berger S, Kunzelmann K, Kriz W, Schütz G, Greger R** 1999 Rescue of the mineralocorticoid receptor knock-out mouse. Pflugers Arch 438:245–254
38. **de Seigneux S, Nielsen J, Olesen ET, Dimke H, Kwon TH, Frøkiaer J, Nielsen S** 2007 Long-term aldosterone treatment induces decreased apical but increased basolateral expression of AQP2 in CCD of rat kidney. Am J Physiol Renal Physiol 293:F87–F99
39. **Le Menuet D, Isnard R, Bichara M, Viengchareun S, Muffat-Joly M, Walker F, Zennaro MC, Lombès M** 2001 Alteration of cardiac and renal functions in transgenic mice overexpressing human mineralocorticoid receptor. J Biol Chem 276:38911–38920
40. **Wang X, Skelley L, Cade R, Sun Z** 2006 AAV delivery of mineralocorticoid receptor shRNA prevents progression of cold-induced hypertension and attenuates renal damage. Gene Ther 13:1097–1103
41. **Quinkler M, Zehnder D, Eardley KS, Lepenies J, Howie AJ, Hughes SV, Cockwell P, Hewison M, Stewart PM** 2005 Increased expression of mineralocorticoid effector mechanisms in kidney biopsies of patients with heavy proteinuria. Circulation 112:1435–1443
42. **Pitt B, Zannad F, Remme WJ, Cody R, Castaigne A, Perez A, Palensky J, Wittes J** 1999 The effect of spironolactone on morbidity and mortality in patients with severe heart failure. Randomized Aldactone Evaluation Study Investigators. N Engl J Med 341:709–717